THE JOURNAL OF BIOLOGICAL CHEMISTRY VOL. 287, NO. 17, pp. 13561–13571, April 20, 2012
Published in the U.S.A.

Activation of Natural Killer T Cells Promotes M2 Macrophage Polarization in Adipose Tissue and Improves Systemic Glucose Tolerance via Interleukin-4 (IL-4)/STAT6 Protein Signaling Axis in Obesity*[S]

Received for publication, February 5, 2012, and in revised form, February 29, 2012 Published, JBC Papers in Press, March 6, 2012, DOI 10.1074/jbc.M112.350066

Yewei Ji[‡], Shengyi Sun[§1], Aimin Xu[¶], Prerna Bhargava[‖], Liu Yang[§], Karen S. L. Lam[¶], Bin Gao[**], Chih-Hao Lee[‖], Sander Kersten[‡‡], and Ling Qi[‡§2]

From the [‡]Division of Nutritional Sciences, [§]Graduate Program in Biochemistry, Molecular and Cell Biology, Cornell University, Ithaca, New York 14853, the [¶]Department of Medicine and Center for Heart, Brain, Hormone, and Healthy Aging, University of Hong Kong, Hong Kong, China, the [‖]Departments of Genetics and Complex Diseases and Nutrition, Harvard University School of Public Health, Boston, Massachusetts 02115, the [**]Laboratory of Liver Diseases, National Institute on Alcohol Abuse and Alcoholism, Rockville, Maryland 20852, and the [‡‡]Nutrition, Metabolism, and Genomics Group, Division of Human Nutrition, Wageningen University, 6700EV, Wageningen, The Netherlands

Background: Obesity is associated with a state of chronic low grade inflammation.
Results: Activation of natural killer T (NKT) cells attenuates inflammation in adipose tissue and improves systemic glucose homeostasis in mice at different stages of obesity.
Conclusion: Upon activation, NKT cells have significant impact on inflammatory responses and systemic glucose tolerance in obesity.
Significance: NKT-activating glycolipids may be useful in treating obesity-associated complications.

Natural killer T (NKT) cells are important therapeutic targets in various disease models and are under clinical trials for cancer patients. However, their function in obesity and type 2 diabetes remains unclear. Our data show that adipose tissues of both mice and humans contain a population of type 1 NKT cells, whose abundance decreases with increased adiposity and insulin resistance. Although loss-of-function of NKT cells had no effect on glucose tolerance in animals with prolonged high fat diet feeding, activation of NKT cells by lipid agonist α-galactosylceramide enhances alternative macrophage polarization in adipose tissue and improves glucose homeostasis in animals at different stages of obesity. Furthermore, the effect of NKT cells is largely mediated by the IL-4/STAT6 signaling axis in obese adipose tissue. Thus, our data identify a novel therapeutic target for the treatment of obesity-associated inflammation and type 2 diabetes.

Natural killer T (NKT)[3] cells have been implicated in autoimmunity, microbial infection, and cancer and hence represent an important immunotherapeutic target (1). Unlike conventional $CD4^+$ and $CD8^+$ T cells, NKT cells recognize and are activated by lipid antigens presented by the MHC class I homologue molecule CD1d on antigen presenting cells such as macrophages and dendritic cells (2–5). Among different types of NKT cells, type 1 or invariant NKT cells are the most abundant and best characterized (6). The prototypical lipid antigen is the marine sponge-derived α-galactosylceramide (αGalCer) (7), which is not found in mammals (7) and has been used widely to specifically study type 1 NKT cells *in vivo* (8). Upon αGalCer activation, NKT cells secrete large amounts of T_H1 cytokine, IFN-γ, and T_H2 cytokines, IL-4 and IL-13 (9). αGalCer challenge has been shown to protect against the development of type 1 diabetes (10) and autoimmune encephalomyelitis (11), although some of these findings remain controversial (8).

The ability of NKT cells to secrete both T_H1 and T_H2 cytokines upon activation underlies their unique regulatory functions that bridge innate and adaptive immunity (8, 12). It is important to note that secretion of T_H1 and/or T_H2 cytokines by NKT cells is context-dependent (8, 12) as the nature of the lipid antigens, the subsets of NKT cells, and the microenvironment of the tissues may have significant influences on their cytokine profiles (11, 13). Indeed, studies have shown that NKT cells may promote or suppress immune processes by skewing adaptive immune responses toward either a T_H1 or T_H2 response (8, 14). However, whether and how NKT cell activation affects obesity-associated inflammation remains to be characterized.

* This work was supported, in whole or in part, by National Institutes of Health Grant R01DK075046 from NIDDK (to C. H. L.) and Grants R01DK082582 and R01DK082582-S1 from NIDDK (to L. Q.). This work was also supported by Hong Kong Collaborative Research Fund Grant HKU4/CRF/10 (to A. X. and K. S. L. L.), Netherlands Nutrigenomics Centre (to S. K.), Cornell startup package, and American Diabetes Association Grants 7-08-JF-47 and 1-12-CD-04.
[S] This article contains supplemental Figs. S1–S7 and Table S1.
[1] Supported by the International Student Research Fellowship from Howard Hughes Medical Institute.
[2] Recipient of the Junior Faculty and Career Development Awards from American Diabetes Association. To whom correspondence should be addressed. Tel.: 607-254-8857; E-mail: lq35@cornell.edu.
[3] The abbreviations used are: NKT, natural killer T; LFD, low fat diet; HFD, high fat diet; HOMA, homeostasis model assessment; GSEA, gene-set enrichment analysis; OGTT, oral glucose tolerance test; WAT, white adipose tissue; BMI, body mass index; αGalCer, α-galactosylceramide; Q-PCR, quantitative PCR; TCR, T cell receptor.

Obesity is associated with a state of chronic low grade inflammation that significantly contributes to the pathogenesis of this disorder and its associated complications. At late stages of obesity, a variety of immune cells, most notably macrophages (15, 16), $CD8^+$ T (17, 18), mast cells (19), B cells (20), and myeloid-derived suppressor cells with immunosuppressive functions (21) infiltrate adipose tissue during diet-induced obesity, with concurrent down-regulation of other immune cells such as regulatory T cells (22). Some of these immune cells may affect the polarization of macrophages to classical (M1) or alternative (M2) activation status via directly or indirectly influencing the local T_H1 or T_H2 cytokines in the adipose microenvironment (23–25). Unlike M1, M2 macrophages may contribute to improved insulin sensitivity due to their capacity to resolve inflammation (*i.e.* anti-inflammation) and facilitate wound healing (25–28). Bias toward M2 polarization can be promoted by immunomodulatory T_H2 cytokines such as IL-4 and IL-13. Studies have identified adipocytes, $CD4^+$ T cells, and eosinophils in adipose tissue as a potential source of T_H2 cytokines (29, 30).

An early study reported the presence of NKT cells in adipose tissue, whose abundance seems decreased with obesity (31). Two recent studies demonstrated the lack of metabolic effect in NKT-deficient *CD1d*$^{-/-}$ mice following long term HFD feeding (32, 33). In light of these results, we asked whether gain-of-function of NKT cells affects obesity-associated glucose homeostasis. Here, we show that αGalCer-mediated activation of NKT cells enhances alternative macrophage polarization in adipose tissue and improves glucose homeostasis in animals at different stages of obesity following the feeding of 60% HFD for 4 days and 8 and 24 weeks. The beneficial effect of NKT cell activation is largely mediated by the IL-4 signaling pathway. Pointing to their significance in human obesity, levels of adipose-resident type 1 NKT cells are found to negatively correlate with BMI, insulin resistance, and fasting glucose levels in humans. As αGalCer is not toxic and is well tolerated in humans (12, 34), our data suggest that NKT-activating glycolipids may be useful in treating obesity-associated type 2 diabetes.

EXPERIMENTAL PROCEDURES

Mouse Models—WT C57/B6 (catalog no. 000664), B6.V-*Lep*^{ob}/J (*ob/ob*, catalog no. 000632), B6.129S6-*Cd1d1/Cd1d2*^{tm1spb}/J (*CD1d*$^{-/-}$, catalog no. 008881), and B6.129P2-*IL4*^{tm1Cgn}/J (*IL-4*$^{-/-}$, catalog no. 002253) were purchased from The Jackson Laboratory and bred at our facility. The latter three have been backcrossed at The Jackson Laboratory to the B6 background over 45, 13, and 12 times, respectively. Myeloid cell-specific PPARγ$^{-/-}$ or PPARδ$^{-/-}$ mice were generated by crossing *Pparg*$^{flox/flox}$ or *Ppard*$^{flox/flox}$ mice to the B6.129P2-*Lyz2*$^{tm1(cre)Ifo}$/J mice (catalog no. 004781, The Jackson Laboratory) (29) and have been backcrossed to the C57BL/6 background over 10 times. Mice were housed in microisolators in our brand new pathogen-free facility with sterile 13% LFD with 13% fat, 67% carbohydrate, and 20% protein from Harlan Teklad (catalog no. 2914) or 60% HFD with 59% fat, 26% carbohydrate, and 15% protein from Bio-Serv Inc. (F3282). All animal procedures were approved by the Cornell and Harvard IACUC.

Human Subjects—39 healthy premenopausal adult Chinese women, including 25 lean individuals with BMI <25 kg/m^2 and 14 overweight/obese subjects with BMI ≥ 25 kg/m^2, undergoing elective abdominal surgery for benign, noninfective gynecological conditions at Queen Mary's hospital, University of Hong Kong, were recruited. Pre-operative assessment was carried out within 1 week of the operation. Anthropometric parameters (body weight, height, waist circumference, and blood pressure) were measured, and body composition was determined by bioelectric impedance analysis (Tanita Body Composition Analyzer TBF-410, Japan). All subjects underwent an oral glucose tolerance test (OGTT) with 75 g of glucose. Fasting plasma glucose and 2-h glucose levels at OGTT were measured by hexokinase method on a Hitachi 747 analyzer (Roche Applied Science). Insulin was measured by microparticle enzyme immunoassay (Abbott). HOMA index was calculated to estimate insulin resistance (IR): HOMA-IR = fasting glucose (mM) × fasting insulin (mIU/liter)/22.5 (35). During the operation, visceral adipose tissues (about 8 cm^3 each) were collected aseptically and transported immediately to the laboratory for RNA extraction and Q-PCR analysis (see below). The study was approved by the Ethics Committee of the University of Hong Kong and adhered to the principles of the Declaration of Helsinki. Written informed consent was obtained from all participants.

Animal Experiments—6-Week-old male mice were fed with either 13% LFD or 60% HFD for an indicated period of time from 4 days to 24 weeks. αGalCer (Toronto Research Chemicals) was dissolved in pyridine at 2.5 mg/ml and then diluted 1:250 in PBS to prepare 10 μg/ml working solution prior to use. In all experiments, mice were injected intraperitoneally with 200 μl of αGalCer (100 ng of αGalCer per g body weight). The vehicle control group was injected with PBS with 0.4% pyridine. The dosage and frequency of αGalCer injection were the same for all the gain-of-function experiments unless indicated. HFD mice were given intraperitoneal αGalCer or vehicle at day 0 and day 2. One day following the GTT (day 4), adipose tissues were harvested, frozen for Q-PCR or Western blot, and fixed for H&E staining. Flow cytometric analyses of NKT levels and other immune cells were performed on day 4. For GTT, mice were fasted for 16–18 h followed by injection of glucose (Sigma) at 1 g/kg body weight. Blood glucose was monitored using One-Touch Ultra Glucometer. Fasting insulin levels were measured following a 6-h fast.

Antibodies and Reagents for Flow Cytometry—Fluorochrome- or biotin-conjugated antibodies against CD3 (145-2C11), TCRβ (H57-597), CD4 (GK1.5), CD8 (YTS169), F4/80 (BM8), CD11b (M1/70), CD45 (30-F11), BrdU-FITC (PRB-1), avidin-PerCP, and isotype control antibodies were purchased from BioLegend, University of California San Francisco Flow Core Facility or BD Biosciences. αGalCer-loaded CD1d-tetramer-phycoerythrin was generously provided by the Tetramer Facility, National Institutes of Health. Data were analyzed using CellQuest software (BD Biosciences) and Flowjo.

Quantitation of Immune Cells in Adipose Tissue Using Flow Cytometric Analysis—Single cell suspensions from stromal vascular cells of adipose tissue were prepared as described (21). Stromal vascular cells from two fat pads per mouse were diluted

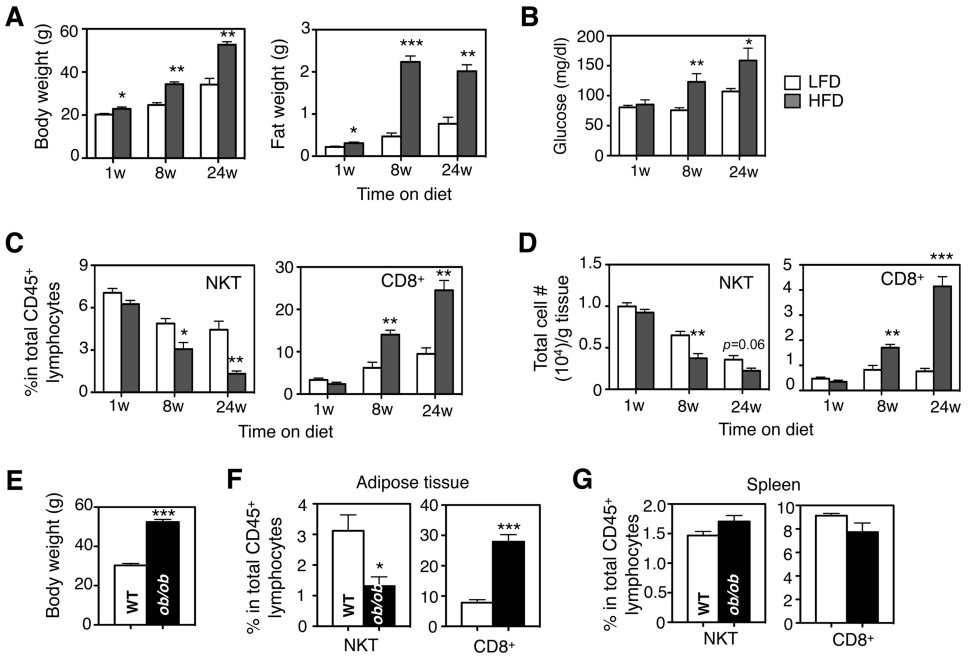

FIGURE 1. **Abundance of adipose NKT cells decreases with HFD feeding in two obese mouse models.** Body, epididymal fat weights (*A*), and fasting glucose levels (*B*) of wild type C57BL/6 male mice under HFD (60%) for 1–24 weeks (*w*) were compared with age-matched male mice on LFD (13% fat). $n = 12–15$ mice each. *C,* percentages of NKT and CD8$^+$ T lymphocytes in total lymphocytes in adipose tissue during HFD feeding compared with age-matched LFD cohort. *D,* total cell numbers of various T lymphocytes per g of adipose tissue during HFD feeding. *C* and *D*, $n = 12$ mice with three repeats. *E,* body weight of adult 36–40-week-old *ob/ob* mice. *F* and *G,* percentages of NKT and CD8$^+$ T cells in adipose tissue (*F*) and spleen (*G*) of *ob/ob* mice compared with age-matched WT lean animals. $n = 10$ mice in each cohort, two repeats. Values represent mean ± S.E. *, $p < 0.05$; **, $p < 0.01$; and ***, $p < 0.005$.

in 120–200 μl of PBS, from which one-tenth was used for the subsequent staining. Following incubation with anti-CD16/CD32 antibody to block Fc receptors, 1×10^6 cells were incubated with 20 μl of antibodies diluted at optimal concentrations for 20 min at 4 °C. Cells were washed three times with PBS and then resuspended in 200 μl of PBS for analysis using the FACSCalibur flow cytometer (BD Biosciences). NKT cells were defined as CD45$^+$ αGalCer-loaded CD1d-tetramer$^+$ CD3/TCRβ^+ lymphocytes (supplemental Fig. S1*A*); CD8$^+$ T cells were defined as CD8$^+$ CD45$^+$ cells (supplemental Fig. S1*B*), and macrophages were as CD45$^+$ F4/80$^+$ CD11b$^+$ cells. During the run, samples were completely run out, and the total number of CD45$^+$ lymphocytes or immune cells was gated and counted. The total cell number for various immune cells per g of adipose tissue was calculated as (% cells in total CD45$^+$ lymphocytes or immune cells × total CD45$^+$ lymphocytes or immune cells)/g of adipose tissue.

Intracellular Flow Cytometric Analysis—For the BrdU staining, mice were injected (intraperitoneally) with αGalCer (100 ng/g of body weight) at day 0 and then with BrdU (Sigma, 0.6 mg/10 g of body weight) at 36 and 12 h prior to sacrifice at day 3. Stromal vascular cells of adipose tissues were purified, labeled with cell surface antibodies, and then fixed in cold 70% ethanol at −20 °C overnight. The rest of steps were performed as the regular flow cytometric analysis using BrdU-FITC antibody and DNA dye 7-aminoactinomycin D (Anaspec).

RNA Extraction and Q-PCR—RNA extraction from cells and murine tissues and Q-PCR were carried out as described previously (36) using TRIzol (Invitrogen) for liver and TRIzol plus QIAeasy kit (Qiagen) for adipose tissues with DNase digestion (Roche Applied Science). Q-PCR data collected on the Light-Cycler 480 (Roche Applied Science) were normalized to ribosomal *l32* gene in the corresponding sample. Primer sequences are listed in supplemental Table S1.

TABLE 1
Clinical characteristics of lean and overweight/obese human subjects recruited in this study
Values are means ± S.E.

	Lean subjects ($n = 25$)	Overweight/obese subjects ($n = 14$)	p value
Age	42.5 ± 7.3 years	44.9 ± 5.6 years	0.089
BMI[a]	21.7 ± 2.1 kg/m^2	28.6 ± 3.3 kg/m^2	<0.001
Fasting glucose[b]	4.7 ± 0.4 mM	4.8 ± 0.5 mM	0.363
2-h glucose[c]	5.8 ± 0.9 mM	7.5 ± 1.0 mM	<0.01
Fasting insulin[b]	3.8 ± 0.6 mIU/liter	5.7 ± 0.9 mIU/liter	0.016
HOMA-IR[d]	1.2 ± 0.2	1.8 ± 0.3	<0.01

[a] BMI is BMI cutoff from lean and overweight/obese is 25.
[b] Fasting glucose/insulin is glucose or insulin levels after an overnight 16-h fast.
[c] 2-h glucose is glucose levels at the end of OGTT, *i.e.* the 2-h time point.
[d] HOMA-IR = (fasting glucose (mM) × fasting insulin (mIU/liter))/22.5.

Analysis of NKT Cells in Human Adipose Tissues by Q-PCR—Following extraction using the Qiagen mini-RNA purification kit, 1 μg of total RNA from each sample was reverse-transcribed. The relative abundance of each gene was determined by Q-PCR on a Prism 7000 sequence detection system (Applied Biosystems) and was normalized against 18 S rRNA. Two primer sets were used to detect NKT cell markers in human adipose tissue; one detects the splicing event of TCR α chain covering the V-J-C rearrangement region with forward primer at *TRAV10* (Vα24, chromosome 14) and reverse primer at *TRAC* (TCR α chain constant region, chromosome 14) (37), and the other detects the use of *TRAV10* (Vα24) (38). A primer set for a common T cell gene *TRBC2* (TCR β chain constant 2, chromosome 7) (38) was included as a control for all T cells. Primer sequences are listed in supplemental Table S1.

Microarray Analysis—Microarray analyses of WAT were performed as described previously (39) and in the supplemental material with four groups ($n = 3–4$ mice each) as follows: WT + vehicle, WT + αGalCer, CD1d$^{-/-}$ + vehicle, and CD1d$^{-/-}$ + αGalCer, all of which were on 4-day HFD feeding with two αGalCer injections at day 0 and day 2. For GSEA, ranking was based on the normalized enrichment score, which reflected the degree to which a gene set in a certain pathway was over-represented at the top (up-regulated) or bottom (down-regulated) of the ranked gene list and was corrected for gene set size. Data have been deposited into the GEO datasets (GSE36032). The array data of IL-4-treated mouse BMDM for 10 days were obtained from the Gene Expression Omnibus (GEO) data base with accession number GSE25088 (40).

Western Blot—Tissues or cells were lysed in Tris-based lysis buffer containing 1% Triton X-100. Normally, 15–30 μg of total lysates, unless otherwise indicated, were used in a mini SDS-PAGE as described (36). Antibodies specific for (Tyr(P)-641) STAT6 and (Tyr(P)-705) STAT3 (Cell Signaling) and arginase 1 (N-20, Santa Cruz Biotechnology catalog no. sc-18351) were used at 1:500–2000, and for the loading control HSP90 (Santa Cruz Biotechnology) was used at 1:6000. The secondary antibody goat anti-rabbit IgG HRP (1:10,000) was from Bio-Rad. Quantitation of band density was carried out using the Image-Lab software of the Bio-Rad ChemiDoc XRS^{+} system following exposure.

H&E Histology—Adipose tissues were fixed in 4% formaldehyde, embedded in paraffin, and sectioned by the Cornell Histology Core Facility. Pictures were taken using the Axiovert 200 M microscope (Zeiss).

ELISA—Blood was collected in animals upon 6 h of fasting during the day. Circulating insulin levels were measured using the kit from Millipore per the supplier's protocols.

Statistical Analysis—Results are expressed as means ± S.E. Comparisons between groups were made using either unpaired two-tailed Student's *t* test of the EXCEL software for two-group comparisons or the one- or two-way analysis of variance test with the Bonferroni post-tests of the PRISM software for multigroup comparisons. For human studies, statistical analysis was performed with the SPSS 11.5 statistical software package. $p < 0.05$ was considered as statistically significant.

RESULTS

Abundance of Adipose-resident Type 1 NKT Decreases with Adiposity in Two Obese Mouse Models—To study the impact of obesity on NKT cells in adipose tissue, we place 6-week-old B6 mice on an HFD containing 60% calories derived from fat or a 13% LFD as a control cohort (supplemental Fig. S1*C*). HFD feeding progressively increased body and epididymal fat pad weights (Fig. 1*A*) as well as fasting glucose levels (Fig. 1*B*). Interestingly, unlike CD8^{+} T cells, abundance of type 1 NKT cells in adipose tissue, in terms of the percentage in total lymphocytes and total cell number per g of adipose tissue, gradually decreased with HFD (Fig. 1, *C* and *D*).

This observation was further confirmed in the adult murine *ob/ob* genetic obesity model; the percentage of NKT cells in adipose tissues was significantly reduced in *ob/ob* mice (Fig. 1, *E* and *F*). The reduction of NKT in adipose tissue of *ob/ob* mice

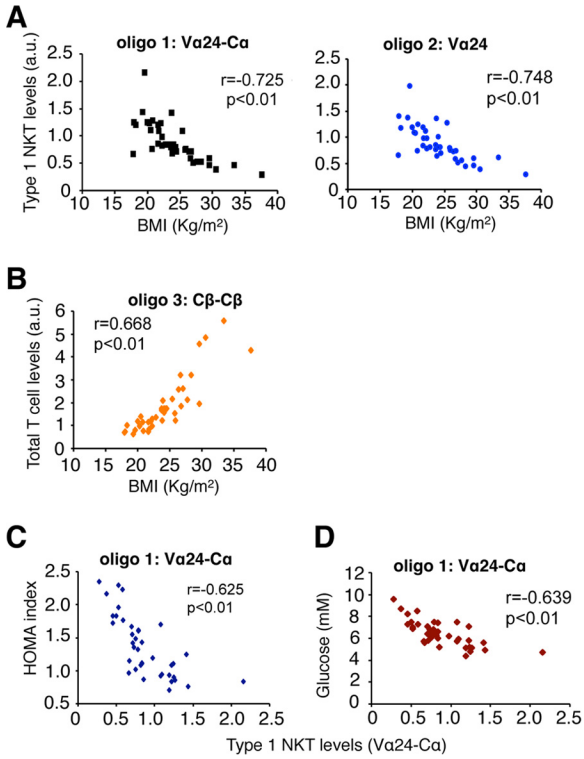

FIGURE 2. **Correlation between adipose NKT cells and metabolic parameters in humans.** Correlations are shown between Vα24 type 1 NKT cells and BMI (*A*), total T cells and BMI (*B*), NKT cells and insulin resistance as measured by HOMA (*C*), and glucose levels measured at the 2-h point of OGTT (*D*). NKT cells in visceral adipose tissues of 39 human subjects were analyzed by two oligonucleotide sets: oligos 1–2 measured the Vα24*TCR* mRNA levels of type 1 NKT cells. A control oligo 3 measured the *TCR* mRNA levels of total T cells. Oligonucleotide positions at the genomic loci of human *TCR* genes and PCR product sizes are shown in supplemental Fig. S2. *a.u.*, arbitrary units.

was not due to defects in NKT cell development or emigration from the thymus as the level of NKT cells in lymphoid organs such as spleen was not affected by obesity (Fig. 1*G*). Taken together, these data suggest that HFD progressively decreases the abundance of NKT cells in adipose tissue.

Levels of Adipose-resident Type 1 NKT Negatively Correlate with Insulin Resistance in Humans—We next analyzed the abundance of NKT cells in visceral adipose tissues collected from 25 lean and 14 overweight/obese Asian female subjects (Table 1). As most CD1d-restricted type 1 human NKT cells express an invariant TCR Vα24 (8, 41, 42), we performed Q-PCR to quantitate the levels of Vα24-containing mRNA or Vα24-associated Vα24-Cα splicing event in adipose tissue (supplemental Fig. S2). Strikingly, Vα24 NKT cells in adipose tissue decreased with BMI (Fig. 2*A*), whereas total T cells (CD4, CD8, and NKT cells) exhibited an opposite trend (Fig. 2*B*). Bivariant correlation analysis further revealed that the levels of Vα24 NKT cells in adipose tissue were inversely correlated with insulin resistance as measured by HOMA index (Fig. 2*C*) and glucose levels at the 2-h point of OGTT (Fig. 2*D*). Thus, the abundance of NKT cells in adipose tissue negatively correlates with BMI, insulin resistance, and fasting glucose in humans.

αGalCer Injection Activates Adipose-resident NKT Cells and Improves Systemic Glucose Homeostasis in Obesity—In line with two recent studies (32, 33), NKT-deficient *CD1d*$^{-/-}$ mice exhibited no changes in glucose tolerance following an 8-week

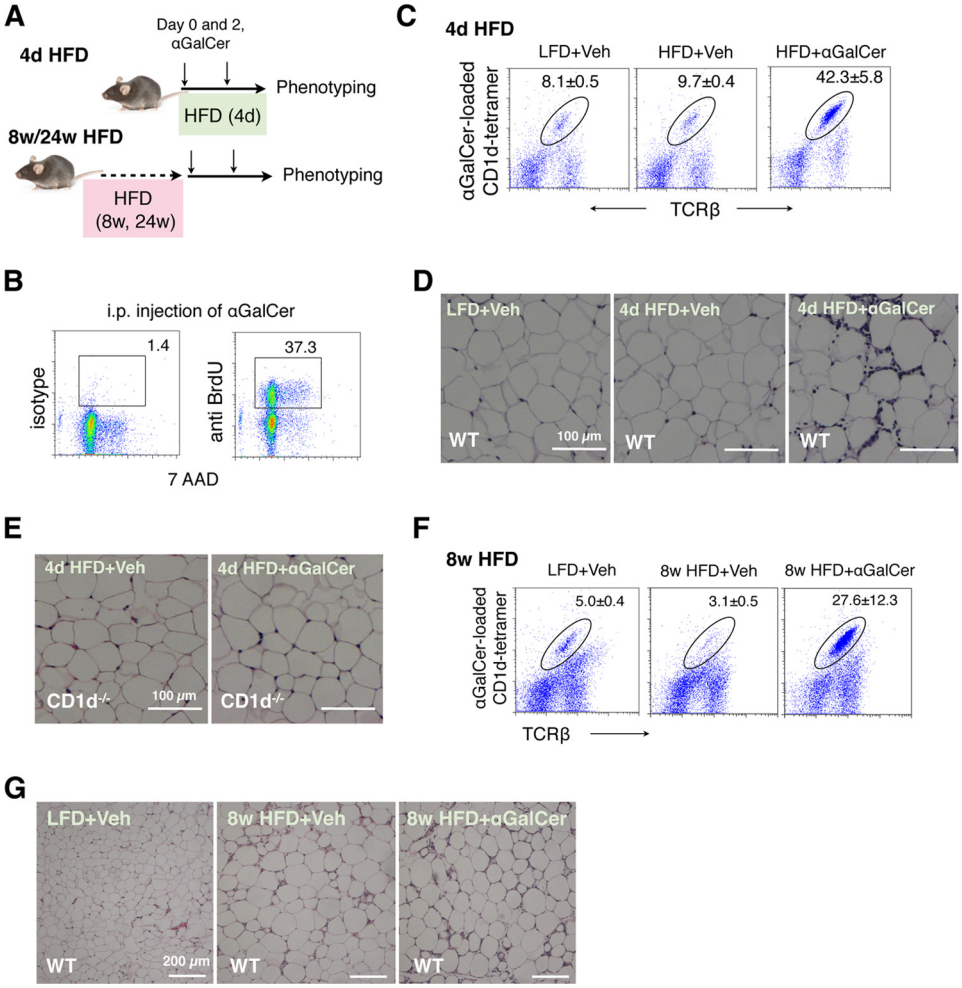

FIGURE 3. **αGalCer challenge activates NKT cells in adipose tissue.** *A,* schematic diagram for three gain-of-function models with 4-day (*d*) and 8- and 24-week HFD feeding. 6-Week-old mice that have been placed on HFD for 4 days and 8 and 24 weeks were injected intraperitoneally with αGalCer or vehicle (*veh*) on day 0 and 2 prior to GTT on day 4 and sacrificed for tissues on day 5. *B,* BrdU labeling of CD1d-tetramer-positive NKT cells in adipose tissue following αGalCer challenge. *7-AAD*, 7-aminoactinomycin D. *C* and *F,* flow analysis of NKT cells in adipose tissue of mice on 4-day (*C*) or 8-week (*F*) HFD. Number refers to the percentage of NKT cells in total CD45$^+$ lymphocytes in stromal vascular cells of adipose tissue. *D* and *E,* H&E section of adipose tissue of WT (*D*) and CD1d$^{-/-}$ (*E*) mice of 4-day HFD. *G,* H&E section of adipose tissue of WT mice of 8-week HFD.

HFD (supplemental Fig. S3*A*). However, to address whether these cells can be targeted therapeutically, we took a gain-of-function approach by stimulating NKT cells *in vivo* with αGalCer. Early studies have established that significant expansion of NKT cells was observed from 2 to 3 days up to 7 days after the initial αGalCer injection, a process associated with sustained cytokine production up to 7 days (43). Accordingly, we challenged HFD-fed male C57BL/6 mice with two αGalCer on days 0 and 2 followed by GTT analysis on day 4 (Fig. 3*A*). To address the therapeutic effect of NKT cell activation at different stages of obesity, we performed these studies in animals that have been on HFD for 4 days and 8 and 24 weeks, which represent short term, long term, and chronic HFD feeding models, respectively.

Indeed, although αGalCer injection had no discernible effect on body and epididymal fat weights (supplemental Fig. S3*B*), it caused massive proliferation of NKT cells in adipose tissue (Fig. 3*B*) with over a 4-fold increase in percentage (Fig. 3*C*) and 70-fold increase in total cell number (supplemental Fig. S4*A*) in 4-day HFD mice. It also caused milder increases of macrophages and CD8$^+$ T cells (supplemental Fig. S4*A*). In line with these observations, H&E staining of WAT sections revealed a significant increase in the number of cells surrounding adipocytes following αGalCer injection (Fig. 3*D*) and were abolished by CD1d deficiency (Fig. 3*E*), suggesting that the expansion of immune cells, including CD8$^+$ T cells and macrophages, is NKT-dependent. Similar observations were made in 8- and 24-week-old HFD mice (Fig. 3, *F* and *G*, and supplemental Figs. S3, *C* and *D*, and S4, *B* and *C*).

Metabolically, αGalCer challenge improved systemic glucose tolerance in mice at all stages of the HFD (Fig. 4, *A–C*) but no effect on fasting insulin levels (Fig. 4*D*). The αGalCer effect on glucose tolerance of HFD mice is NKT cell-dependent as it had no effect in *CD1d*$^{-/-}$ mice (Fig. 4*E*). Pointing to the importance of HFD in NKT cell effect, αGalCer injection in mice on LFD had no effect on glucose tolerance (Fig. 4*F*). Thus, NKT cell activation by αGalCer improves systemic glucose tolerance in obese animals.

Activation of NKT Cells Enhances M2 Macrophage Polarization in Adipose Tissue—To explore possible mechanisms underlying the beneficial effect of NKT cell activation, we assessed the inflammatory status of adipose tissue by examining the status of macrophage polarization. αGalCer challenge caused a marked 50–100-fold induction of a subset of M2 genes

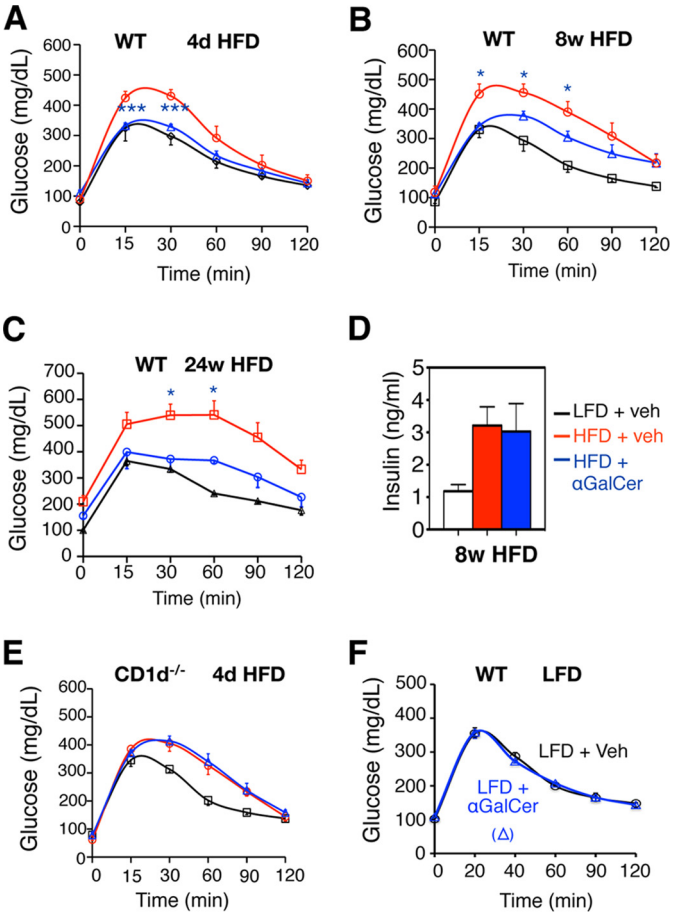

FIGURE 4. **NKT cell activation improves systemic glucose homeostasis in diet-induced obesity mice.** *A–C,* GTT of WT mice on LFD or HFD injected with vehicle (*veh*) or αGalCer. *A,* $n = 12–15$ mice each cohort with three repeats; *B,* $n = 9–10$ mice of each cohort with two repeats; *C,* $n = 3–4$ mice per HFD cohort and $n = 10$ mice for LFD. * refers to the p values compared between HFD + vehicle (*veh*) and HFD + αGalCer groups. *D,* fasting insulin levels in mice under 8-week HFD. $n = 9–10$ mice each, two repeats. *E,* GTT of CD1d$^{-/-}$ mice on LFD or HFD injected with vehicle (*veh*) or αGalCer. $n = 9–10$ mice each cohort with two repeats. *F,* GTT of WT mice on LFD with vehicle or αGalCer injection. $n = 10$ mice each, two repeats. Values represent mean ± S.E. *, $p < 0.05$, and ***, $p < 0.005$.

in adipose tissue in an NKT-dependent manner, including *Arg1*, *Chi3l3*, and *Pdcd1lg2*, and to a much lesser extent M1 genes in all three HFD models (Fig. 5, *A* and *B* and supplemental Fig. S5*A*). This observation was further supported by the protein level of a key M2 macrophage marker; Arg1 protein was significantly induced in response to αGalCer in WT WAT but abolished in *CD1d*$^{-/-}$ WAT (Fig. 5, *C* and *D*). Intriguingly, this effect was limited to adipose tissue not in the liver (supplemental Fig. S5*B*). Thus, we conclude that NKT cell activation by αGalCer promotes M2 polarization in adipose tissue in obesity.

What mediates the NKT cell effect in adipose tissue? To address this question, we performed a nonbiased microarray analysis to study the global impact of αGalCer injection on gene expression in mice (supplemental Fig. S6*A*). As αGalCer effects on macrophage polarization were similar among all three diet-induced obesity models (Fig. 5, *A* and *B*, and supplemental Fig. S5*A*), we performed array analysis in adipose tissues harvested from the 4-day HFD model, where a relatively higher signal-to-noise ratio was anticipated compared with that of long term HFD. Indeed, the expression of 1556 genes was significantly increased by more than 2-fold in an absolute NKT-dependent manner (Fig. 6*A*). GSEA indicated pronounced induction of many pathways related to immune functions, including the "T_H1/T_H2 differentiation" and the "IL-4 pathway" (supplemental Fig. S6*B*). In comparison with a pre-existing dataset (40), we found that 40% of genes up-regulated by IL-4 in macrophages were also induced by αGalCer in WAT (Fig. 6*C*). Furthermore, most components of the canonical IL-4 signaling pathway were induced by αGalCer in WAT (supplemental Fig. S6*C*). Pointing to a potential role of IL-4, 7 of the top 10 αGalCer-induced genes in WAT were also highly up-regulated in IL-4-treated macrophages (40), and many were classical M2 genes such as *Chi3l3* (138-fold, αGalCer *versus* vehicle in WT WAT), *pdcd1lg2* (53-fold), and *Arg1* (32-fold) (Fig. 6*B*).

The array data were further supported by Q-PCR and Western blot analyses of Arg1 levels of WAT (Figs. 5*A* and 6, *D* and *E*). Providing direct support for the elevated IL-4 signaling in WAT, *Il4* mRNA levels in WAT were highly induced by αGalCer treatment in an NKT-dependent manner (Fig. 6*F*). Thus, we conclude that αGalCer-mediated NKT cell activation increases IL-4 signaling in adipose tissue.

NKT Cell Effect Is Mediated by the IL-4/STAT6 Signaling Axis in Adipose Tissue—We next determined the physiological importance of IL-4 in αGalCer-mediated NKT cell activation using *IL-4*$^{-/-}$ mice. Although both body and adipose weights were comparable among WT and *IL-4*$^{-/-}$ cohorts following 4-day HFD (Fig. 7*A*), loss of IL-4 completely abolished the αGalCer effect in glucose tolerance (Fig. 7, *B* and *C*) and reduced the total number of infiltrating immune cells in adipose tissue following αGalCer injection (supplemental Fig. S7*A*). Indeed, total lymphocytes in WAT of *IL-4*$^{-/-}$ mice were reduced by ~40% relative to WT cohorts (supplemental Fig. S7*B*).

Loss of IL-4 markedly attenuated the αGalCer-mediated induction of M2 genes *Arg1*, *Chi3l3*, and *Pdcd1lg2* (Fig. 7*D*) and Arg1 protein in WAT (Fig. 7, *E* and *F*). Moreover, loss of IL-4 completely abolished tyrosine phosphorylation (Tyr(P)) of STAT6 but not Tyr(P) of STAT3, in WAT following αGalCer-mediated NKT activation (Fig. 7, *E* and *F*). Providing further support to the significance of adipose tissue in mediating NKT effect *in vivo*, hepatic STAT6 was not activated by αGalCer (Fig. 7*G*).

Finally, it has been shown that the IL-4/STAT6 effect may be mediated by the activities of nuclear receptors (PPARγ or PPARβ/δ) in macrophages (44). However, αGalCer-mediated induction of M2 genes was not affected in WAT of myeloid cell-specific *PPARγ* or *PPARβ/δ*-deficient animals when compared with WT control littermates (supplemental Fig. S7*C*). Thus, NKT cells regulate macrophage polarization and exert metabolic control largely through the IL-4/STAT6 axis in obese adipose tissue, in a PPARγ- and PPARβ/δ-independent manner.

DISCUSSION

Our understanding of the role of NKT cells in regulating obesity-associated inflammation remains incomplete. Our data using mice fed with a 60% HFD for 8 weeks confirmed the findings of two previous reports where no metabolic effect was seen in CD1d$^{-/-}$ mice upon feeding of 45 or 60% HFD for 26 or

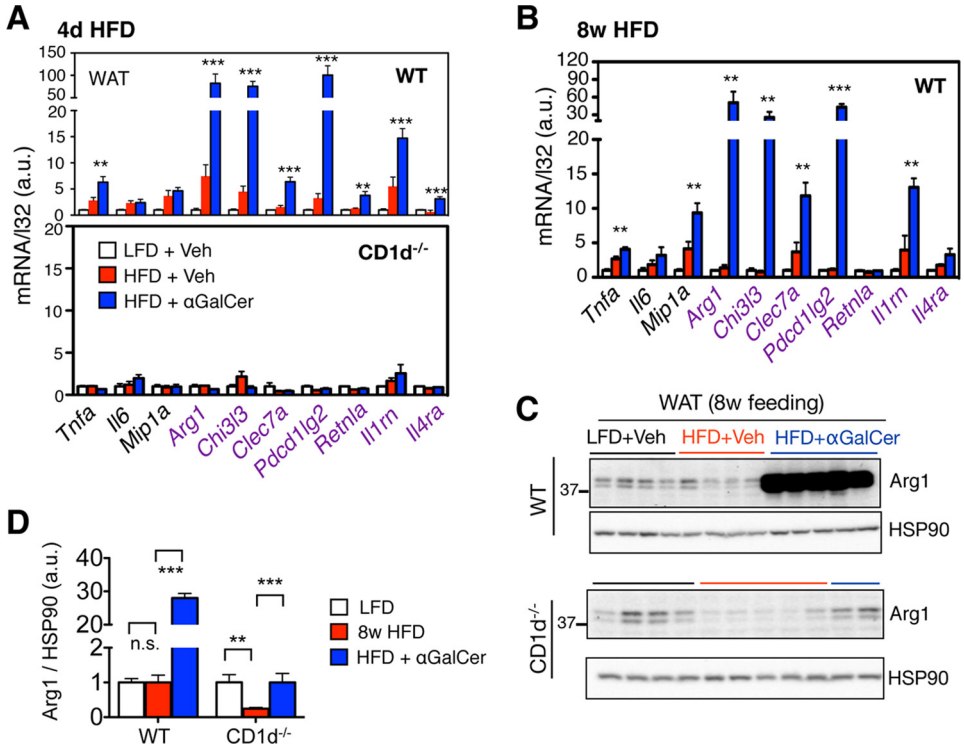

FIGURE 5. **NKT cell activation increases M2 polarization in adipose tissue of diet-induced obesity mice.** *A,* Q-PCR analysis of M1 (*black*) and M2 genes (*purple*) in WAT of WT (*upper*) and CD1d$^{-/-}$ mice (*lower*) of 4-day HFD mice. $n = 10–15$ mice each cohort with 2–3 experiments. *B,* Q-PCR analysis of M1 (*black*) and M2 genes (*purple*) in WAT of 8-week HFD mice. $n = 4–5$ mice per cohort, two repeats. *C* and *D,* Western blot analysis of Arg1 expression in WAT of WT and CD1d$^{-/-}$ cohorts with vehicle or αGalCer treatment. $n = 3–4$ mice each, two repeats. Each lane represents an independent sample. Quantitation shown in *D*, with the values of the LFD + vehicle sample set at 1. Values represent mean ± S.E. *n.s.* not significant. **, $p < 0.01$, and ***, $p < 0.005$. *a.u.*, arbitrary units.

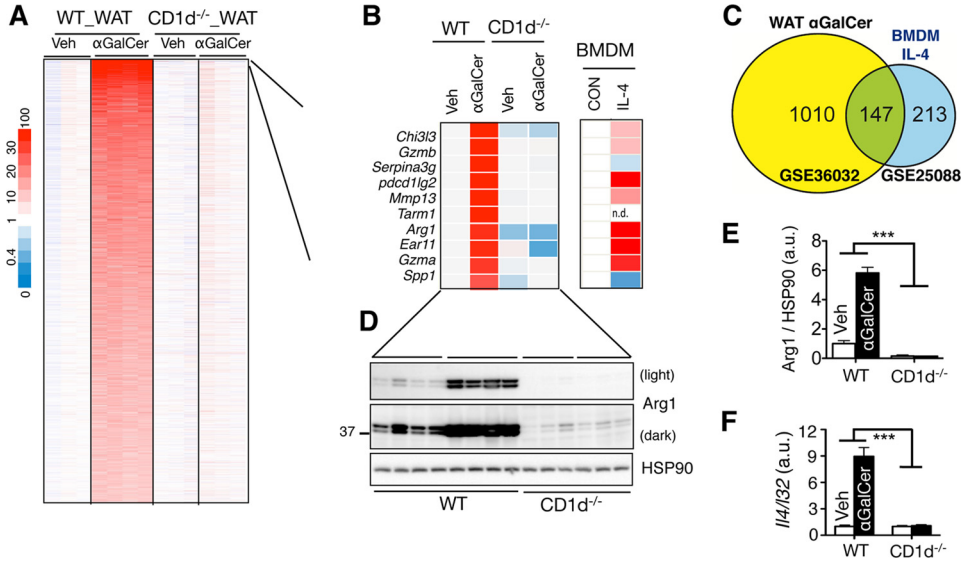

FIGURE 6. **NKT cell activation increases IL-4 signaling in adipose tissue.** *A,* heat map showing the fold-change of gene expression in WAT of WT or CD1d$^{-/-}$ mice on 4-day HFD with or without αGalCer injection. $n = 3–4$ mice each. A total of 1556 differentially expressed genes with $q < 0.001$ and fold-change >2 are shown. *B,* top 10 genes up-regulated by αGalCer and their expression changes in IL-4-treated BMDM (GSE25088). *n.d.*, not detected. *Veh*, vehicle; *CON*, control. *C,* Venn diagrams showing the overlap of significantly up-regulated genes in αGalCer-injected WAT *versus* IL-4-treated BMDM data sets. As not all αGalCer-induced genes existed in the IL-4_BMDM dataset, only 1157 genes, rather than 1556 genes induced by αGalCer, were included in the Venn diagrams. *D,* Western blot analysis of Arg1 expression in WAT of WT and CD1d$^{-/-}$ cohorts under 4-day HFD with vehicle or αGalCer treatment. $n = 3–4$ mice each, two repeats. Each lane represents an independent sample. Quantitation shown in *E* with the values of the WT + vehicle sample set at 1. *F,* Q-PCR analysis of *Il4* mRNA levels in WAT of WT or CD1d$^{-/-}$ mice on 4-day HFD with or without αGalCer injection. $n = 4$ mice each. Values represent mean ± S.E. ***, $p < 0.005$. *a.u.*, arbitrary units.

8–16 weeks (32, 33). These loss-of-function studies suggest that NKT cells are dispensable for glucose homeostasis at chronic obesity. In contrast, our gain-of-function study demonstrated that αGalCer-mediated NKT cell activation promotes M2 macrophage polarization and exerts a salutary effect on systemic glucose homeostasis through the IL-4/STAT6 signaling axis. These gain-of-function data are in line with the known function of NKT cells in altering T_H1/T_H2 responses *in*

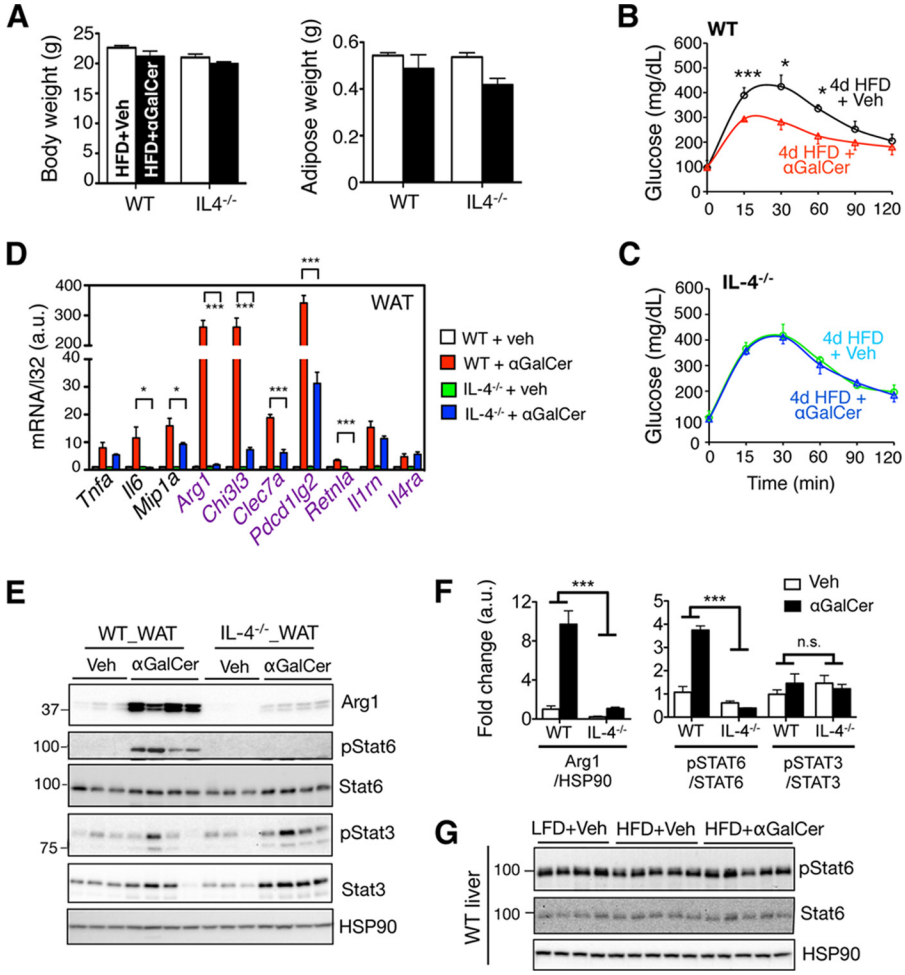

FIGURE 7. **NKT cell activation signals through the IL-4/STAT6 axis in adipose tissue.** 6–7-Week-old mice were placed on either LFD or HFD for 4 days with two αGalCer or vehicle (*Veh*) injections prior to metabolic phenotyping. *A,* weights of body and epididymal adipose tissues. *B* and *C,* GTT, $n = 7–8$ mice each cohort with two repeats. *D,* Q-PCR analysis of M1 and M2 genes in WAT. $n = 6$ mice each cohort with two repeats. *E* and *F,* Western blot analysis of Arg1, (Tyr(P)) STAT6 and (Tyr(P)) STAT3 in WAT of WT and IL-4$^{-/-}$ mice ($n = 3–5$ mice each cohort with two repeats). The ratios of Arg1 to HSP90, Tyr(P) STAT3/6 to total STAT3/6 were quantitated in *F. G,* Western blot analyses of Tyr(P) STAT6 proteins in the liver of the WT mice under 4-day HFD with or without αGalCer injection ($n = 4–5$ mice each). Each lane represents an independent sample. Values represent mean ± S.E. *, $p < 0.05$; **, $p < 0.01$; ***, $p < 0.005$; *n.s.*, not significant; *a.u.*, arbitrary units.

vivo (8). The lack-of-effect of NKT cells at late stages of obesity in the absence of stimulation is not surprising given the massive infiltration and expansion of other cells such as CD8$^+$ T cells and macrophages (23, 24) and given the concomitant reduction of NKT cells (Fig. 1). Thus, these studies suggest that in the absence of a strong agonist, NKT cell effect in adipose tissue in the context of obesity is limited and may be dispensable; however, upon activation by a potent stimulus such as αGalCer, NKT cells have significant impact on inflammatory responses in adipose tissue and systemic glucose tolerance in obese animals.

Using the β_2-microglobulin-deficient mice that lack all MHC class I molecules, including CD1d, a recent study concluded that NKT cells infiltrate adipose tissue and that loss of NKT cells reduces inflammation in obesity, whereas activation of NKT cells by one injection of αGalCer had mild effect on glucose tolerance in HFD animals (45), opposite to our findings. However, interpretation of their results is confounded by the fact that the β_2-microglobulin knock-out mice not only are deficient in NKT but also CD8$^+$ T cells (46, 47). Accordingly, the absence of CD8$^+$ T cells may account for the reported phenotypes (18).

In line with the role of IL-4 in T_H2 responses, our data suggest the IL-4 is an important mediator of NKT cell function in adipose tissue in the context of obesity. However, it does not exclude the role of other T_H2 cytokines such as IL-13, which is known to be secreted by NKT cells (9). This is supported by our observation that loss of IL-4 only partially blocked αGalCer-mediated induction of M2 genes in adipose tissue (Fig. 7*D versus* 5*A*). Although IL-4 and IL-13 share a common signaling pathway through the IL-4 receptor α subunit (IL-4Rα), they may have diverse functions *in vivo*. Studies have shown that repression of tumor immunosurveillance by NKT cells was mediated via IL-13 rather than IL-4 (48). Therefore, the role of IL-13 in NKT cell function in obesity needs to be further delineated by using the IL-13 knock-out mice.

Our observation that, unlike their hepatic counterparts, adipose-resident NKT cells have a T_H2-biasing effect upon αGalCer activation is very intriguing. The difference may be related to the nature of antigen presenting cells, tissue microen-

vironment, and/or the different lineage of NKT cells in adipose tissue (8). Our preliminary data showed that unlike $CD4^+$ $CD8^-$ NKT cells in the liver, the majority of NKT cells in adipose tissue are $CD4^-$ $CD8^-$,[4] and thus may be associated with specific functional changes. Indeed, earlier studies have shown that $CD4^-$ $CD8^-$ *versus* $CD4^+$ $CD8^-$ NKT cells likely represent functionally separate lineages that may promote different T_H response with distinct capacities to secrete T_H1 and T_H2 cytokines (8, 49–51). Alternatively, the tissue-specific NKT effect may reflect a unique microenvironment of adipose tissue in terms of antigen presenting cells. Intriguingly, as adipocytes express CD1d transcript (data not shown), they may be able to present lipids to and directly activate NKT cells, whereas Kupffer cells in the liver have been shown to be important for αGalCer-mediated NKT cell activation (52). Finally, as NKT cell activation by bacterial lipid antigens may be toll-like receptor 4-dependent and IL-12-mediated (53, 54), it will be interesting to investigate whether different cytokine environments of the liver *versus* adipose tissue may explain the tissue-specific NKT effect upon αGalCer activation.

Our data show that αGalCer-mediated NKT activation leads to activation of the IL-4/STAT6 signaling axis in adipose tissue, promoting M2 macrophage polarization. How IL-4 mediates macrophage polarization in adipose tissue remains unclear. It has been shown that STAT6 may modulate the activities of nuclear receptors (PPARγ or PPARβ/δ) (44) or induce the expression of histone H3K27 demethylase Jmjd3 (encoded by *Kdm6b* gene) (55, 56) to influence M2 macrophage polarization. Our data show that M2 marker genes induced by αGalCer are not affected by lack of either PPARγ or PPARβ/δ in myeloid cells, consistent with two recent studies demonstrating that PPARγ and PPARβ/δ in macrophages or myeloid cells are dispensable for the T_H2 responses (40, 57). The discrepancies may be due to different genetic backgrounds of mice, fatty acid composition of diets, or gut microbiota. It will be interesting to delineate whether the combined actions of PPARγ and PPARβ/δ or more intriguingly epigenetic regulation by Jmjd3 may be required for the NKT cell effect in adipose tissue. Additionally, besides its effect on macrophage polarization, IL-4 may affect differentiation of naive T cells and B cells. In light of recent studies showing important roles of various T and B cells in the pathogenesis of obesity (18, 20), the interplay among different cell types in obese adipose tissue is an interesting area of future studies.

In line with the animal data, the abundance of type 1 NKT cells in adipose tissue decreases in obese humans. Although this was initially reported by an earlier study (31), our data using a much larger cohort further demonstrate that abundance of type 1 NKT cells in adipose tissue negatively correlates with BMI, insulin resistance, and OGTT glucose levels. The near-perfect correlations between adipose NKT and metabolic parameters suggest that these cells may be involved in the regulation of insulin sensitivity in obese humans. As αGalCer is not toxic and is well tolerated in humans and often stimulates the expansion of residual NKT cell populations in other disease settings (12, 34), our data suggest that NKT-activating glycolipids may have clinical application in treating type 2 diabetes. Therapies using NKT lipid agonists may skew T_H2 bias in adipose tissue and hence delay or ameliorate the development of inflammation and type 2 diabetes in obese patients. Further studies are required to determine the optimal dosage, feeding routes, and frequency of αGalCer or other T_H2-biasing lipid agonists in humans.

Acknowledgments—We thank Dr. Mark Boekschoten (Wageningen University) for help with the microarray analysis and members of the Qi laboratory for technical assistance and insightful discussions, and we are very grateful to the National Institutes of Health Tetramer Facility, Emory University, for the generous supply of the αGalCer-loaded CD1d tetramers.

REFERENCES

1. Cerundolo, V., Silk, J. D., Masri, S. H., and Salio, M. (2009) Harnessing invariant NKT cells in vaccination strategies. *Nat. Rev. Immunol.* **9,** 28–38
2. Bendelac, A., Lantz, O., Quimby, M. E., Yewdell, J. W., Bennink, J. R., and Brutkiewicz, R. R. (1995) CD1 recognition by mouse $NK1^+$ T lymphocytes. *Science* **268,** 863–865
3. Bendelac, A. (1995) Positive selection of mouse $NK1^+$ T cells by CD1-expressing cortical thymocytes. *J. Exp. Med.* **182,** 2091–2096
4. Porcelli, S., Morita, C. T., and Brenner, M. B. (1992) CD1b restricts the response of human $CD4-8^-$ T lymphocytes to a microbial antigen. *Nature* **360,** 593–597
5. Beckman, E. M., Porcelli, S. A., Morita, C. T., Behar, S. M., Furlong, S. T., and Brenner, M. B. (1994) Recognition of a lipid antigen by CD1-restricted $\alpha\beta^+$ T cells. *Nature* **372,** 691–694
6. Godfrey, D. I., Stankovic, S., and Baxter, A. G. (2010) Raising the NKT cell family. *Nat. Immunol.* **11,** 197–206
7. Kawano, T., Cui, J., Koezuka, Y., Toura, I., Kaneko, Y., Motoki, K., Ueno, H., Nakagawa, R., Sato, H., Kondo, E., Koseki, H., and Taniguchi, M. (1997) CD1d-restricted and TCR-mediated activation of vα14 NKT cells by glycosylceramides. *Science* **278,** 1626–1629
8. Bendelac, A., Savage, P. B., and Teyton, L. (2007) The biology of NKT cells. *Annu. Rev. Immunol.* **25,** 297–336
9. Yoshimoto, T., Bendelac, A., Watson, C., Hu-Li, J., and Paul, W. E. (1995) Role of $NK1.1^+$ T cells in a TH2 response and in immunoglobulin E production. *Science* **270,** 1845–1847
10. Hong, S., Wilson, M. T., Serizawa, I., Wu, L., Singh, N., Naidenko, O. V., Miura, T., Haba, T., Scherer, D. C., Wei, J., Kronenberg, M., Koezuka, Y., and Van Kaer, L. (2001) The natural killer T-cell ligand α-galactosylceramide prevents autoimmune diabetes in non-obese diabetic mice. *Nat. Med.* **7,** 1052–1056
11. Miyamoto, K., Miyake, S., and Yamamura, T. (2001) A synthetic glycolipid prevents autoimmune encephalomyelitis by inducing TH2 bias of natural killer T cells. *Nature* **413,** 531–534
12. Berzins, S. P., Smyth, M. J., and Baxter, A. G. (2011) Presumed guilty. Natural killer T cell defects and human disease. *Nat. Rev. Immunol.* **11,** 131–142
13. Bai, L., Sagiv, Y., Liu, Y., Freigang, S., Yu, K. O., Teyton, L., Porcelli, S. A., Savage, P. B., and Bendelac, A. (2009) Lysosomal recycling terminates CD1d-mediated presentation of short and polyunsaturated variants of the NKT cell lipid antigen αGalCer. *Proc. Natl. Acad. Sci. U.S.A.* **106,** 10254–10259
14. Kronenberg, M. (2005) Toward an understanding of NKT cell biology. Progress and paradoxes. *Annu. Rev. Immunol.* **23,** 877–900
15. Weisberg, S. P., McCann, D., Desai, M., Rosenbaum, M., Leibel, R. L., and Ferrante, A. W. (2003) Obesity is associated with macrophage accumulation in adipose tissue. *J. Clin. Invest.* **112,** 1796–1808
16. Xu, H., Barnes, G. T., Yang, Q., Tan, G., Yang, D., Chou, C. J., Sole, J.,

[4] Y. Ji, S. Sun, L. Yang, X. Li, X. Sheng, S. Kersten, and L. Qi, unpublished data.

Nichols, A., Ross, J. S., Tartaglia, L. A., and Chen, H. (2003) Chronic inflammation in fat plays a crucial role in the development of obesity-related insulin resistance. *J. Clin. Invest.* **112,** 1821–1830
17. Rausch, M. E., Weisberg, S., Vardhana, P., and Tortoriello, D. V. (2008) Obesity in C57BL/6J mice is characterized by adipose tissue hypoxia and cytotoxic T-cell infiltration. *Int. J. Obes.* **32,** 451–463
18. Nishimura, S., Manabe, I., Nagasaki, M., Eto, K., Yamashita, H., Ohsugi, M., Otsu, M., Hara, K., Ueki, K., Sugiura, S., Yoshimura, K., Kadowaki, T., and Nagai, R. (2009) $CD8^+$ effector T cells contribute to macrophage recruitment and adipose tissue inflammation in obesity. *Nat. Med.* **15,** 914–920
19. Liu, J., Divoux, A., Sun, J., Zhang, J., Clément, K., Glickman, J. N., Sukhova, G. K., Wolters, P. J., Du, J., Gorgun, C. Z., Doria, A., Libby, P., Blumberg, R. S., Kahn, B. B., Hotamisligil, G. S., and Shi, G. P. (2009) Genetic deficiency and pharmacological stabilization of mast cells reduce diet-induced obesity and diabetes in mice. *Nat. Med.* **15,** 940–945
20. Winer, D. A., Winer, S., Shen, L., Wadia, P. P., Yantha, J., Paltser, G., Tsui, H., Wu, P., Davidson, M. G., Alonso, M. N., Leong, H. X., Glassford, A., Caimol, M., Kenkel, J. A., Tedder, T. F., McLaughlin, T., Miklos, D. B., Dosch, H. M., and Engleman, E. G. (2011) B cells promote insulin resistance through modulation of T cells and production of pathogenic IgG antibodies. *Nat. Med.* **17,** 610–617
21. Xia, S., Sha, H., Yang, L., Ji, Y., Ostrand-Rosenberg, S., and Qi, L. (2011) $Gr\text{-}1^+$ $CD11b^+$ myeloid-derived suppressor cells suppress inflammation and promote insulin sensitivity in obesity. *J. Biol. Chem.* **286,** 23591–23599
22. Feuerer, M., Herrero, L., Cipolletta, D., Naaz, A., Wong, J., Nayer, A., Lee, J., Goldfine, A. B., Benoist, C., Shoelson, S., and Mathis, D. (2009) Lean, but not obese, fat is enriched for a unique population of regulatory T cells that affect metabolic parameters. *Nat. Med.* **15,** 930–939
23. Olefsky, J. M., and Glass, C. K. (2010) Macrophages, inflammation, and insulin resistance. *Annu. Rev. Physiol.* **72,** 219–246
24. Donath, M. Y., and Shoelson, S. E. (2011) Type 2 diabetes as an inflammatory disease. *Nat. Rev. Immunol.* **11,** 98–107
25. Gordon, S., and Martinez, F. O. (2010) Alternative activation of macrophages. Mechanism and functions. *Immunity* **32,** 593–604
26. Lumeng, C. N., Bodzin, J. L., and Saltiel, A. R. (2007) Obesity induces a phenotypic switch in adipose tissue macrophage polarization. *J. Clin. Invest.* **117,** 175–184
27. Odegaard, J. I., Ricardo-Gonzalez, R. R., Red Eagle, A., Vats, D., Morel, C. R., Goforth, M. H., Subramanian, V., Mukundan, L., Ferrante, A. W., and Chawla, A. (2008) Alternative M2 activation of Kupffer cells by PPARδ ameliorates obesity-induced insulin resistance. *Cell Metab.* **7,** 496–507
28. Odegaard, J. I., Ricardo-Gonzalez, R. R., Goforth, M. H., Morel, C. R., Subramanian, V., Mukundan, L., Red Eagle, A., Vats, D., Brombacher, F., Ferrante, A. W., and Chawla, A. (2007) Macrophage-specific PPARγ controls alternative activation and improves insulin resistance. *Nature* **447,** 1116–1120
29. Kang, K., Reilly, S. M., Karabacak, V., Gangl, M. R., Fitzgerald, K., Hatano, B., and Lee, C. H. (2008) Adipocyte-derived Th2 cytokines and myeloid PPARδ regulate macrophage polarization and insulin sensitivity. *Cell Metab.* **7,** 485–495
30. Wu, D., Molofsky, A. B., Liang, H. E., Ricardo-Gonzalez, R. R., Jouihan, H. A., Bando, J. K., Chawla, A., and Locksley, R. M. (2011) Eosinophils sustain adipose alternatively activated macrophages associated with glucose homeostasis. *Science* **332,** 243–247
31. Lynch, L., O'Shea, D., Winter, D. C., Geoghegan, J., Doherty, D. G., and O'Farrelly, C. (2009) Invariant NKT cells and $CD1d^+$ cells amass in human omentum and are depleted in patients with cancer and obesity. *Eur. J. Immunol.* **39,** 1893–1901
32. Kotas, M. E., Lee, H. Y., Gillum, M. P., Annicelli, C., Guigni, B. A., Shulman, G. I., and Medzhitov, R. (2011) Impact of CD1d deficiency on metabolism. *PLoS ONE* **6,** e25478
33. Mantell, B. S., Stefanovic-Racic, M., Yang, X., Dedousis, N., Sipula, I. J., and O'Doherty, R. M. (2011) Mice lacking NKT cells but with a complete complement of $CD8^+$ T-cells are not protected against the metabolic abnormalities of diet-induced obesity. *PLoS ONE* **6,** e19831
34. Giaccone, G., Punt, C. J., Ando, Y., Ruijter, R., Nishi, N., Peters, M., von Blomberg, B. M., Scheper, R. J., van der Vliet, H. J., van den Eertwegh, A. J., Roelvink, M., Beijnen, J., Zwierzina, H., and Pinedo, H. M. (2002) A phase I study of the natural killer T-cell ligand α-galactosylceramide (KRN7000) in patients with solid tumors. *Clin. Cancer Res.* **8,** 3702–3709
35. Matthews, D. R., Hosker, J. P., Rudenski, A. S., Naylor, B. A., Treacher, D. F., and Turner, R. C. (1985) Homeostasis model assessment: insulin resistance and beta-cell function from fasting plasma glucose and insulin concentrations in man. *Diabetologia* **28,** 412–419
36. Sha, H., He, Y., Chen, H., Wang, C., Zenno, A., Shi, H., Yang, X., Zhang, X., and Qi, L. (2009) The IRE1α-XBP1 pathway of the unfolded protein response is required for adipogenesis. *Cell Metab.* **9,** 556–564
37. Kis, J., Engelmann, P., Farkas, K., Richman, G., Eck, S., Lolley, J., Jalahej, H., Borowiec, M., Kent, S. C., Treszl, A., and Orban, T. (2007) Reduced $CD4^+$ subset and Th1 bias of the human iNKT cells in type 1 diabetes mellitus. *J. Leukocyte Biol.* **81,** 654–662
38. Vijayanand, P., Seumois, G., Pickard, C., Powell, R. M., Angco, G., Sammut, D., Gadola, S. D., Friedmann, P. S., and Djukanovic, R. (2007) Invariant natural killer T cells in asthma and chronic obstructive pulmonary disease. *N. Engl. J. Med.* **356,** 1410–1422
39. Lichtenstein, L., Mattijssen, F., de Wit, N. J., Georgiadi, A., Hooiveld, G. J., van der Meer, R., He, Y., Qi, L., Köster, A., Tamsma, J. T., Tan, N. S., Müller, M., and Kersten, S. (2010) Angptl4 protects against severe proinflammatory effects of saturated fat by inhibiting fatty acid uptake into mesenteric lymph node macrophages. *Cell Metab.* **12,** 580–592
40. Szanto, A., Balint, B. L., Nagy, Z. S., Barta, E., Dezso, B., Pap, A., Szeles, L., Poliska, S., Oros, M., Evans, R. M., Barak, Y., Schwabe, J., and Nagy, L. (2010) STAT6 transcription factor is a facilitator of the nuclear receptor PPARγ-regulated gene expression in macrophages and dendritic cells. *Immunity* **33,** 699–712
41. Lantz, O., and Bendelac, A. (1994) An invariant T cell receptor α chain is used by a unique subset of major histocompatibility complex class I-specific $CD4^+$ and $CD4-8^-$ T cells in mice and humans. *J. Exp. Med.* **180,** 1097–1106
42. Dellabona, P., Padovan, E., Casorati, G., Brockhaus, M., and Lanzavecchia, A. (1994) An invariant Vα24-JαQ/Vβ11 T cell receptor is expressed in all individuals by clonally expanded $CD4-8^-$ T cells. *J. Exp. Med.* **180,** 1171–1176
43. Wilson, M. T., Johansson, C., Olivares-Villagómez, D., Singh, A. K., Stanic, A. K., Wang, C. R., Joyce, S., Wick, M. J., and Van Kaer, L. (2003) The response of natural killer T cells to glycolipid antigens is characterized by surface receptor down-modulation and expansion. *Proc. Natl. Acad. Sci. U.S.A.* **100,** 10913–10918
44. Chawla, A. (2010) Control of macrophage activation and function by PPARs. *Circ. Res.* **106,** 1559–1569
45. Ohmura, K., Ishimori, N., Ohmura, Y., Tokuhara, S., Nozawa, A., Horii, S., Andoh, Y., Fujii, S., Iwabuchi, K., Onoé, K., and Tsutsui, H. (2010) Natural killer T cells are involved in adipose tissues inflammation and glucose intolerance in diet-induced obese mice. *Arterioscler. Thromb. Vasc. Biol.* **30,** 193–199
46. Koller, B. H., Marrack, P., Kappler, J. W., and Smithies, O. (1990) Normal development of mice deficient in β2M, MHC class I proteins, and $CD8^+$ T cells. *Science* **248,** 1227–1230
47. Zijlstra, M., Bix, M., Simister, N. E., Loring, J. M., Raulet, D. H., and Jaenisch, R. (1990) β_2-Microglobulin-deficient mice lack $CD4-8^+$ cytolytic T cells. *Nature* **344,** 742–746
48. Terabe, M., Matsui, S., Noben-Trauth, N., Chen, H., Watson, C., Donaldson, D. D., Carbone, D. P., Paul, W. E., and Berzofsky, J. A. (2000) NKT cell-mediated repression of tumor immunosurveillance by IL-13 and the IL-4R-STAT6 pathway. *Nat. Immunol.* **1,** 515–520
49. Lee, P. T., Benlagha, K., Teyton, L., and Bendelac, A. (2002) Distinct functional lineages of human V(α)24 natural killer T cells. *J. Exp. Med.* **195,** 637–641
50. Benlagha, K., Kyin, T., Beavis, A., Teyton, L., and Bendelac, A. (2002) A thymic precursor to the NK T cell lineage. *Science* **296,** 553–555
51. Pellicci, D. G., Hammond, K. J., Uldrich, A. P., Baxter, A. G., Smyth, M. J., and Godfrey, D. I. (2002) A natural killer T (NKT) cell developmental pathway involving a thymus-dependent $NK1.1^-CD4^+$ CD1d-dependent

precursor stage. *J. Exp. Med.* **195,** 835–844
52. Schmieg, J., Yang, G., Franck, R. W., Van Rooijen, N., and Tsuji, M. (2005) Glycolipid presentation to natural killer T cells differs in an organ-dependent fashion. *Proc. Natl. Acad. Sci. U.S.A.* **102,** 1127–1132
53. Brigl, M., Bry, L., Kent, S. C., Gumperz, J. E., and Brenner, M. B. (2003) Mechanism of CD1d-restricted natural killer T cell activation during microbial infection. *Nat. Immunol.* **4,** 1230–1237
54. Brigl, M., Tatituri, R. V., Watts, G. F., Bhowruth, V., Leadbetter, E. A., Barton, N., Cohen, N. R., Hsu, F. F., Besra, G. S., and Brenner, M. B. (2011) Innate and cytokine-driven signals, rather than microbial antigens, dominate in natural killer T cell activation during microbial infection. *J. Exp. Med.* **208,** 1163–1177
55. Ishii, M., Wen, H., Corsa, C. A., Liu, T., Coelho, A. L., Allen, R. M., Carson, W. F., 4th, Cavassani, K. A., Li, X., Lukacs, N. W., Hogaboam, C. M., Dou, Y., and Kunkel, S. L. (2009) Epigenetic regulation of the alternatively activated macrophage phenotype. *Blood* **114,** 3244–3254
56. Satoh, T., Takeuchi, O., Vandenbon, A., Yasuda, K., Tanaka, Y., Kumagai, Y., Miyake, T., Matsushita, K., Okazaki, T., Saitoh, T., Honma, K., Matsuyama, T., Yui, K., Tsujimura, T., Standley, D. M., Nakanishi, K., Nakai, K., and Akira, S. (2010) The Jmjd3-Irf4 axis regulates M2 macrophage polarization and host responses against helminth infection. *Nat. Immunol.* **11,** 936–944
57. Marathe, C., Bradley, M. N., Hong, C., Chao, L., Wilpitz, D., Salazar, J., and Tontonoz, P. (2009) Preserved glucose tolerance in high fat-fed C57BL/6 mice transplanted with PPAR$\gamma^{-/-}$, PPAR$\delta^{-/-}$, PPAR$\gamma\delta^{-/-}$, or LXR$\alpha\beta^{-/-}$ bone marrow. *J. Lipid Res.* **50,** 214–224